Webology, Volume 18, Number 5, 2021
ISSN: 1735-188X
DOI: 10.29121/WEB/V18I5/30

GIS Investigation on the Electrical Emission and Mobility of Conducting Particles

Ashutosh Dixit[1], Sandeep Sunori[2]

[1]Department of Electrical Engineering, Graphic Era Deemed to be University, Dehradun, Uttarakhand India, 248002
[2]Department of Electronics & Communication Engineering, Graphic Era Hill University, Bhimtal, Uttarakhand India, 263156

ABSTRACT

As a result of loose intermetallic phases in the circuit protection switchboard, electrical charge deformation occurs, resulting in leakage and subsequent failure within that GIS. Under various working circumstances, sequential metals of different amounts as well as numerals were also placed in the exact role of 126kV GIS. These same leakage waves are created by the Wideband procedure, as well as an elevated webcam is employed to research this same mobility as well as acoustic emission features of various intermetallic phases in GIS. Examine its movement patterns. The starting discharging power, frequency of fires, and proportional charge intensity achieved are examined, as well as the findings reveal that over freely rotating intermetallic phases, the discharging magnitude, measured flow magnitude, and discharging timings are all the same. The maximum output volume remained constant, appreciably after the power was raised. The observed flow loudness as well as the frequency of episodes fell initially and later rose. The amount of bash grew with subatomic particle size after this leap. This same release magnitude is positively related to the development of releases, as well as particulate duration, as well as inversely related to stress, and the measured flow magnitude things tend to inundate to increasing scrutiny; in GIS, there are three methods of inter-particulate motion; the measured flow perceived loudness, the measured flow loudness, and the measured flow loudness. There is a favourable relationship.

Keywords: GIS Investigation; Electrical Emission; Breakdown; Amplitude; Discharge Voltage.

INTRODUCTION

Except for its benefits in terms of space, energy impacts, insulating effectiveness, and so on, ArcGIS is therefore extensively associated with the production of elevated distributed generation. Alloying elements were unavoidably formed during manufacturing, assembling, as well as operating of GIS, like unsanitary glass shards during industrial processes as well as ionic compounds created by contacting movements throughout operations. Loose microparticles are a prevalent problem that accounts for at least 38% of any and all insulating losses with Arcgis [1]. Amongst these, the insulated nanoparticles will receive a small metallic layer off their surfaces during air electron transfer, causing them to act like intermetallic phases while posing no significant danger to the GIS's

Webology, Volume 18, Number 5, 2021
ISSN: 1735-188X
DOI: 10.29121/WEB/V18I5/30

insulator capability. Underneath the Iris hole, the alloying elements were revealed. Vibrating easily inside the skin can cause adhesion to an anode surface as well as the interface of an insulator, lowering the overall insulating grade of a GNSS. As a result, studying the motion laws or leakage behaviour of particulate reinforcement in ArcGIS is critical [2,3].

Researchers at local and international levels have conducted substantial thermodynamic studies on the mobility patterns as well as discharge properties of straight nanoparticles. The criteria are provided by Li Dajian and colleagues from Sichuan. College students studied the movement of both round and longitudinal nanoparticles among flat plate actuators. Researchers felt that the flying periods of straight nanoparticles were higher compared to microspheres, but scientists could never investigate the impact of longitudinal component lengths upon viral movement behaviour. A Snao K et al. did model and experimental analysis just on particles' movement laws inside an unequal magnetic charge [4].

Khan Y et al. investigated the mobility of intermetallic phases close to an insulator at DC power, but did not examine the velocity profile close to an isolator during voltage level. Researcher Qi Bor of North Central Electricity Supply Academy employed VHF technologies to detect a fault induced by longitudinal intermetallic phases on the surfaces of an actual dielectric. Their findings confirmed that now the discharges progress over 3 parts, and the hazard of intermetallic phases may be efficiently determined by fault current properties. An earlier study employed a plate anode technique to test the link between metallic nanoparticles with dielectric breakdown starting potential, but this does not establish a particular criterion. Numerous studies examined the discharging parameters of nanoparticles mounted on the elevated buses, enclosures, as well as insulation, utilising the genuine 510kV Arcgis as that of the integration prototype. Liu Sihua from North Central Electricity Supply College as well as colleagues investigated the link between the quantity of leakage of nanoparticles in Ac circuits as well as particulate height, but could not investigate the impact of analyte concentration [5,6].

The preceding research investigated the mobility of loose metal shavings as well as the features of leakage as well as associated affecting variables, but there was no examination of the effect of analyte concentration inside the air-conditioning GPs. Throughout this study, a Hf approach is employed to detect faults, as well as a 130kV fuel added flexibility is built. Rectangular metal atoms of variable lengths as well as amounts are placed in various areas of a GIS. Combine electrical fire signals and particulate mobility.

EXPERIMENTAL WORK

2.1 Experimental Platform

Its research employs genuine 126kVGIS research equipment to investigate the mobility of metal shards inside the Gis cavities as well as accurately depict the properties of GIS leakage. Some of these include this same perimeter of a concertmaster wire R1 = 60 mm, this same having a diameter of something like the residential R2 = 220 mm, and all the exploratory cavity's fuel surroundings establishing; all these parties of a chamber also seem to be monitoring doors encased in translucent crystal, as well as a shoulder monitoring screen is utilised to complement the lamp and employ an elevated webcam to notice this same movement behaviour of intermetallic phases within the

Webology, Volume 18, Number 5, 2021
ISSN: 1735-188X
DOI: 10.29121/WEB/V18I5/30

chamber. The VHF sensors are positioned just on the losing side of the interval of 30 minutes, where they are employed for synchronised true leakage signal detection and therefore are linked to a laptop, enabling experimentation processing and storing. Figure 1 depicts the GIS experimentation system. The microparticles employed in the investigation were straight aluminium strands having radiuses of 0.3 mm as well as lengths of 2.5 mm, 5 mm, 7.5 mm, and 10 mm.

2.2 Experimental Method

Besides being pressed to a particular input power, the freed mercury vapours lift off again after collecting energy just on grounding electrodes as well as commence to repeat, discharging to a connector as well as grounding electrodes in motion. For just an instance, consider a flattened rectangular metallic particle with a length of 12mm. Immerse it in a chamber with something like a 0.5 MPa pressure drop. Whenever the load changes to 38kV, these nanoparticles begin to rise strongly as well as haphazardly move across the longitudinal axis. As demonstrated in Figure 2, the overall pounding rate of intermetallic phases travelling inside the path of a dielectric steadily decreases while it does not change. Whenever travelling towards a barrier, electrons would bind to it and stop walking, increasing the pounding speed of intermetallic phases travelling away first from the insulating layer. There might be mobility inside the reverse way, such that to the position of an isolator, but no substantial alterations will take place.

RESULT AND DISCUSSION

3.1 Particle Movement and Discharge Phenomenon

At the start of the experiment, a linearly metallic powder was inserted vertically inside the chamber, as well as the location of the exam particles, which were maintained constant every session. Its GPS was therefore evacuated and completely refilled using clean Sf6. Gradually raise the power inside the experimentation container till a steady leakage indication develops, then pressurise once per hour using 1 kV/min steps. Following that, the nanoparticles jumped and the cameras were used to continuously capture their velocity for ten seconds while using VHF measuring instruments. Analyse the discharging sound wave on a continuing basis. Because these VHF signals could now calibrate the actual discharge region, the transmitter intensity was used to define the device magnitude of a leakage quantity, and the measurement was in Volts. Changes in the size of the metal shards, ambient air velocity, and the amount of intermetallic phases placed inside the cavities were used to make measurements, and each set of experiments was repeated multiple times [7].

3.1.2 Discharge Phenomenon.

Pictures 3, 4, and 5 depict the most recent experimental developments of a discharging volume, measured flow loudness, and drug release increasing power using 1 minute as the statistics timeframe, while The following figure shows the process run spectra. Following achieving this discharged initiating potential, the discharging magnitude, observed flow loudness, and frequency of discharged also rise only with an increase in the load, particularly rapidly before achieving the tio2 nanoparticles turn power output. When the sample power was raised, the discharging intensity multiplied by 1.5 times and the frequency of discharged grew by approximately 4-5 times. However, the measured flow intensity as well as the number of releases were not affected considerably [8,9].

Webology, Volume 18, Number 5, 2021
ISSN: 1735-188X
DOI: 10.29121/WEB/V18I5/30

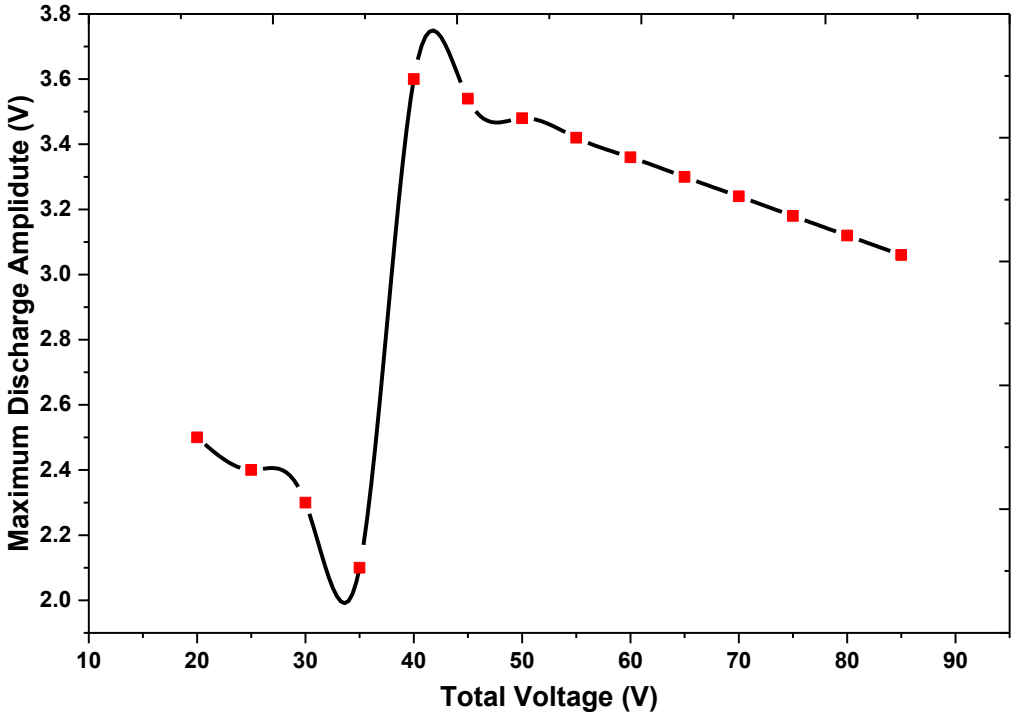

Fig.1. Development of Trend on Maximum discharge

It lowers initially, then rises, and the rising pattern of a measured flow magnitude is identical to what it was prior to the intermetallic phases taking off. Half of the input shocks are now more parallel inside the process automatic methods pattern, which does impact an electricity provider's fields distortions inside the GPS cavities. Electrons happen following electron collisions as well as refrigerant collisions in locations with such a strong amplitude. A continual discharging connection can be made by the simultaneous effect of heavy ions, yield, as well as thermal ionisation.

Electrostatic pressure, Lorenz power, electromagnetic field pressure differences, and certain other pressures occur between electrified metallic particles. A metallic reaction occurs if the strain is strong. If the substances travel gradually towards the insulators, they can attach to an insulator's human body due to voltages collected just on the insulating material, posing various risks to the proper functioning of GPS. While in research, when the power grows beyond optimum hoisting potential, the electricity distribution potential inside the Gds grows as well, leading to an increased release intensity as well as a frequency of explosions. Any mobility of intermetallic phases since being pressured to the raising potential would intensify the method and result in continual leakage [10,11].

Webology, Volume 18, Number 5, 2021
ISSN: 1735-188X
DOI: 10.29121/WEB/V18I5/30

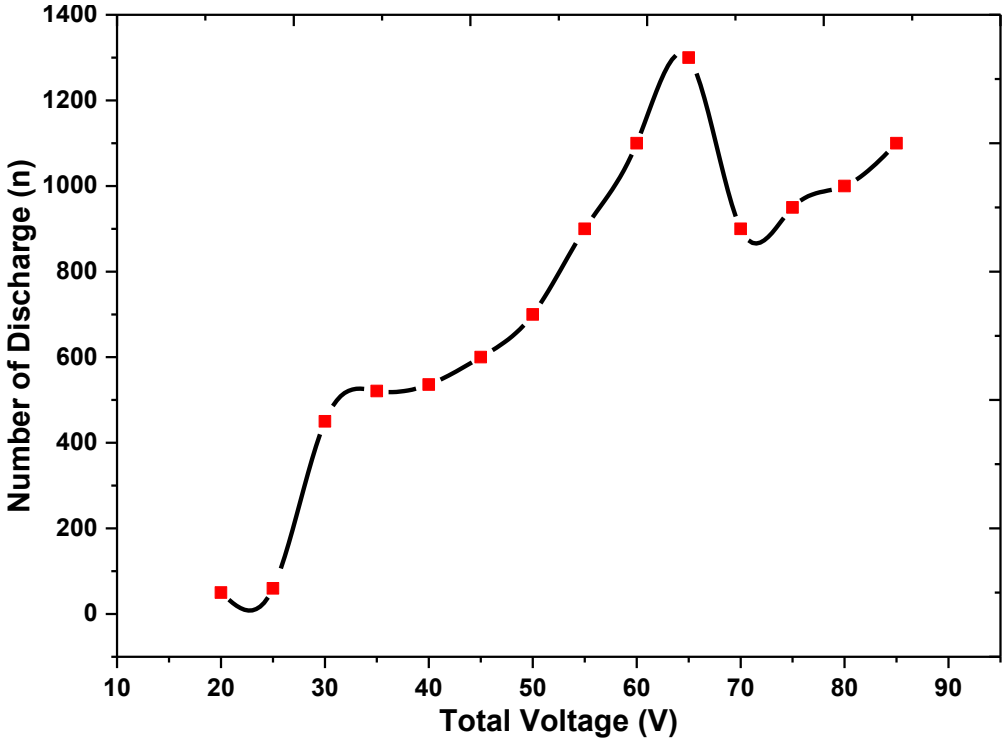

Fig.2. Development of Trend on discharge time

Whenever the metallic electrons flow, the unevenness of their electrical potential changes proportionally. Whenever the localised electrostatic force just at the nanoparticles' position is inadequate to keep the microparticles migrating, the nanoparticles cease trying to move, decreasing the fault. Because the electromagnetic field disruption induced by particulate displacement persists, the leakage persists and it is much more intense than when the energy is reduced. As a result, whenever the hoisting energy hits 38kV, its highest fault current intensity, measured flow loudness, and total frequency of releases also skyrocket. The mercury vapours stabilised as well as adsorption on insulating material over time, and also the particulate matter occurrence really did not reoccur after the output was expanded. The electromagnetic field deformation induced by atoms remained, therefore the phase margin of leakage didn't reflect markedly after a huge rise. Whenever the nanoparticles keep beating, the frequency and discharge as well as median intensity of releases decrease quickly, but slowly increase as power increases.

Various quantities of straight intermetallic phases with just a width of 3mm and a diameter of 0.3mm were placed inside the research chamber to evaluate the consequences of various quantities of rectangular fragments on the motion as well as discharging behaviours of nanoparticles. To evaluate the basic mobility behaviour features of many straight nanoparticles, consider inserting two-dimensional atoms. Whenever the energy reached 51kV, one of the straight atoms leapt dramatically. About 3 separate movement sequences occurred at about this time. Figure 10 depicts Option 1. (a). A metallic particle which leaps initially goes in the path of its own turn, while the other metallic particles don't seem to. Figure 10 depicts Option 2. (b). Whenever one edge of a particle comes into contact with some other metal nanoparticle, some other metal atoms will rise as

Webology, Volume 18, Number 5, 2021
ISSN: 1735-188X
DOI: 10.29121/WEB/V18I5/30

well as travel rapidly. These two aluminium nanoparticles travel in the exact same directions, but the space separating them grows. Figure 10 depicts option 3 (c), Once one side of a first metal nanoparticle reaches second metallic particles, the other metal particles climb up as they travel aggressively upward inside the primary quantum state motion. Whenever the quantity of intermetallic phases is increased to either three or four, its activity remains the same as if there are just metal nanoparticles [12].

CONCLUSION

In GIS, when exposed to power, loose mercury vapours start to arbitrarily hop across the longitudinal axis, generating leakage indications. Upon attaining a discharging initiating power, the discharging magnitude, observed flow loudness, and frequency of explosions depend on the initial output power. It will happen abruptly upon attaining the hoisting potential but before attaining the beginning potential of a metal shard. Following this, as the experimental power climbed, its total cycle magnitude remained unchanged. However, the measured flow intensity as well as the frequency of discharged decreased initially, but subsequently grew. This frequency of leaps inside 10s after some alloying elements are removed will reach a high point, mostly as powder diameter as well as velocity rise. The reduction as well as saturate trends show that even as component height grows, electron discharges get increasingly powerful.

REFERENCES

1. Sun, L.; Fan, X.; Jiang, S.; Wang, B.; Liu, Y.; Gao, S.; Meng, L. Study on Electrical Aging Characteristics of Fiber Sheath Materials in Power Transformer Oil. J. Electr. Eng. Technol. 2019, 14, 323–330, doi:10.1007/s42835-018-00041-5.
2. Vittal, M.M.K.P. DC Fault Protection in Multi - Terminal VSC - Based HVDC Transmission Systems with Current Limiting Reactors. J. Electr. Eng. Technol. 2019, doi:10.1007/s42835-018-00027-3.
3. Cheol, W.; Dong, L.; Hwang, H. Improved SSJ - MPPT Method for Maximum Power Point Tracking of Photovoltaic Inverter Under Partial Shadow Condition. J. Electr. Eng. Technol. 2019, doi:10.1007/s42835-018-00018-4.
4. Symp, M. © 2004 WILEY-VCH Verlag GmbH & KGaA, Weinheim DOI: 10.1002/Masy.200451314. 2004, 179–190, doi:10.1002/masy.200451314.
5. Arias, A.C.; Mackenzie, J.D.; Mcculloch, I.; Rivnay, J.; Salleo, A. Materials and Applications for Large Area Electronics : Solution-Based Approaches. 2010, 3–24.
6. Jae, H.; Dong, L.; Kim, E.; Geun, J.; Jae, S.; Park, D.; Park, J.D. Switchboard Fire Detection System Using Expert Inference Method Based on Improved Fire Discrimination. J. Electr. Eng. Technol. 2019, 14, 1007–1015, doi:10.1007/s42835-019-00092-2.
7. Fu, Q.; Peng, L.; Li, L.; Lin, M.; Zhao, Y.; Li, S.; Chen, C. Detection of Methanol in Power Transformer Oil Using Spectroscopy. 2019, doi:10.1007/s42835-019-00097-x.
8. Al, Q.A.; Mohd, G.; Mohd, A. Dynamic Security Assessment for Power System Under Cyber - Attack. J. Electr. Eng. Technol. 2019, 14, 549–559, doi:10.1007/s42835-019-00084-2.
9. Faris, M.; Izzah, B.; Zakaria, H.; Hafizi, M.; Aulia, A.; Nawawi, Z. Effect of Surfactant on Breakdown Strength Performance of Transformer Oil - Based Nanofluids. J. Electr. Eng. Technol. 2019, 14, 395–405, doi:10.1007/s42835-018-00028-2.

Webology, Volume 18, Number 5, 2021
ISSN: 1735-188X
DOI: 10.29121/WEB/V18I5/30

10. Hyun, K. Evaluation of a Content - Based Image Retrieval Computer - Aided Diagnosis System for Breast Ultrasound Images Through Distance Similarity Measures. J. Electr. Eng. Technol. 2019, doi:10.1007/s42835-018-00003-x.
11. Qiu, H.; Zhao, X.; Yang, C.; Ran, Y.; Wei, Y. Influence of Inter - Turn Short - Circuit Fault Considering Loop Current on Electromagnetic Field of High - Speed Permanent Magnet Generator with Gramme Ring Windings. J. Electr. Eng. Technol. 2019, 14, 701–710, doi:10.1007/s42835-019-00122-z.
12. Awang, M.; Ismail, H.Ã.; Hazizan, M.A. ARTICLE IN PRESS POLYMER Processing and Properties of Polypropylene-Latex Modified Waste Tyre Dust Blends (PP / WTD ML). 2008, 27, 93–99, doi:10.1016/j.polymertesting.2007.09.008.